

## A HIGH PRECISION PWM TRANSCONDUCTANCE AMPLIFIER FOR MICROSTEPPING USING UNITRODE'S UC3637

### INTRODUCTION

If you ask a designer why he has chosen a stepping motor for a given application, chances are that his answer will include something about "open loop positioning." Stepping motors can provide accurate positioning without expensive position sensors and feedback loops, and this fact alone results in large savings.

But there is more: steppers are tough and durable, easy to use, and high in power rate. And if you want to close a feedback loop around them, you can do that, too.

Still, there are certain problems. Steppers are *incremental motion* machines, and as such they tend to be noisy and

are prone to behave erratically under certain conditions; for example, when the stepping rate is such as to excite a mechanical or electro-mechanical resonant mode. Furthermore, although the angular increments may be small—especially when half-stepping is used—the positioning resolution is restricted to a finite number of discrete points.

Therefore, this question arises: "Is there a method of driving stepping motors such that the resulting movement is smooth and quiet—that is, essentially continuous, as opposed to incremental? And would this result in improved positioning resolution?" We will try to answer these questions here.

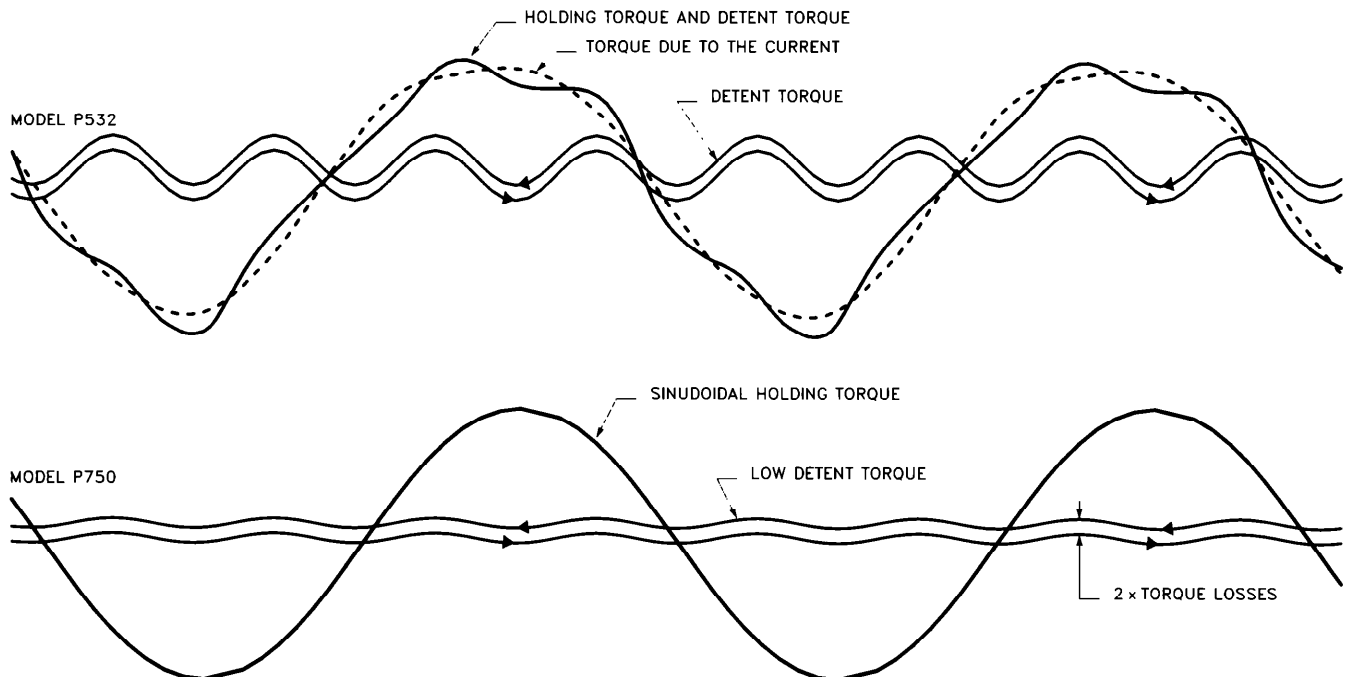


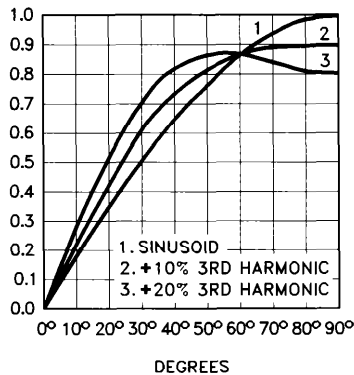
Figure 1. Static Torque Curves of Two Hybrid Steppers

### STATIC TORQUE CURVES

The curves in Figure 1 illustrate how a stepping motor torque behaves as a function of rotor angle. The detent torque component is a consequence of the magnetic field produced by the rotor magnet (or magnets), and is present with or without phase currents applied. It can be seen that this component contributes a fourth harmonic distortion to the static torque curves. The energized torque curves, in general, have additional harmonic components, mostly the third and fifth. Note that the two motors depicted

in Figure 1 have very different characteristics in this respect. The distortion observed in the static torque characteristic is of no great consequence in the more usual applications of stepping motors, using either full step or half step sequences. It is when we start thinking about increasing the positioning resolution of these motors by some method of apportioning currents between the two phases, that we begin to be concerned about the effects of harmonic distortion. Even small amounts of added har-

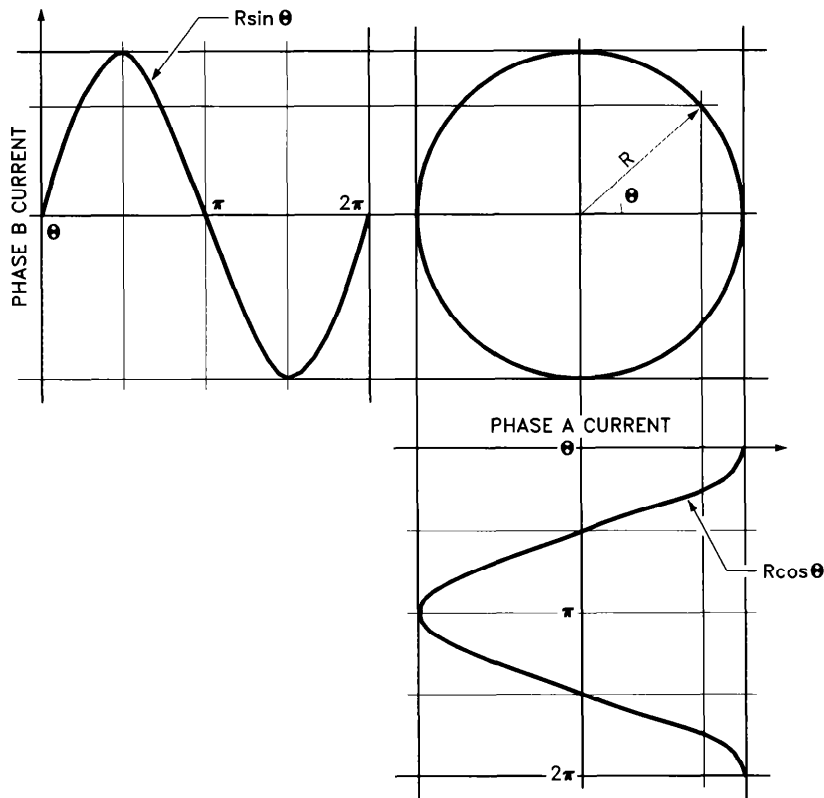
monics can have a very noticeable effect on the wave-shape, as shown in Figure 2.



0017-2

Figure 2. Effect of 10% and 20% Harmonic Content

Figure 3 shows the relationship between sine and cosine waveforms, and what it tells us is that if we can get a motor with a sinusoidal static torque characteristic-i.e., with no harmonic components-and drive phase A with a sine current function and phase B with a cosine current function, we would have smooth shaft rotation and accurate positioning at any angle.



0017-3

Figure 3. The sum of sine and cosine waveforms is a smoothly rotating vector.

Stepping motors having static torque curves with very low harmonic distortion are commercially available today. But most low-priced, mass produced hybrid steppers exhibit torque curves with enough harmonic components to require careful consideration in any attempt to improve resolution by what is known as *microstepping*. (The name *microstepping* originates from the fact that the required current waveforms are generated by a digital process that approximates those waveforms incrementally. With thirty-two or sixty-four increments for an electrical angle of  $\pi/2$  radians, the resulting waveforms are hardly distinguishable from true sine or cosine signals.)

If the nonsinusoidal static characteristic of a given motor is known, it is possible to generate appropriate wave-shapes for the phase currents so that the resulting torque curve becomes free of distortion, as required. Note that this involves no additional complexities, since it is just as easy-or difficult-to synthesize one waveform as another. Consequently, one can, in principle, linearize any motor for increased resolution and smoothness through microstepping.

Still, it should be noted that the best efficiency is obtained when the phase current waveshapes are undistorted, because of all suitable waveforms, the sine wave has the lowest form-factor.

The form-factor of a waveform is the ratio of its rms to average values. For a sine wave, this ratio is:

$$(1) \text{ff}_S = \frac{0.707}{0.637} = 1.111$$

Some manufacturers have used triangular waveforms—largely because they can be implemented with great simplicity—and it is interesting to note that for such a waveform, the average value is  $0.5 V_{PK}$ , while the rms is  $0.577 V_{PK}$ . Thus the form factor is:

$$(2) \text{ff}_T = \frac{0.577}{0.5} = 1.155$$

As a consequence, for the same peak power applied to the motor, the rms power of a triangular waveform is 18% less than that of a sine wave, whereas the average current is 21% less. It follows that microstepping with a triangular waveform does not use the full capabilities of the motor.

The same result is obtained with other-waveforms, as long as the peak power is limited, as it must be.

But regardless of all this, the fact remains that whether our motor has a sinusoidal torque curve or a very distorted one, the thing that will be inevitably required will be two amplifiers capable of converting the synthesized waveform into phase currents *at the required power levels*. In the next section, we will describe the design of one such amplifier, having a transconductance linearity of better than 1% and capable of delivering phase currents of up to  $\pm 6A$ .

### UNITRODE'S UC3637 PWM CONTROLLER

Pulse width modulation (PWM) is a method of power control whose most attractive feature is the high level of efficiency that can be obtained. With careful design, and using power MOSFETs as output switches, one can easily achieve efficiencies higher than 80%.

The Unitrode UC3637 PWM controller, housed in an eighteen-pin DIL package, was originally intended to serve as a PWM amplifier for brush-type PM servomotors. But, because of its ingenious design, the device has found its way into various other uses as well, such as temperature control, uninterruptible power supplies, and even high fidelity sound reproduction. As we shall see, it can also be used in a high performance PWM transconductance amplifier.

### BLOCK DIAGRAM AND LOOP EQUATIONS

A block diagram of the current feedback loop under consideration is shown in Figure 4, where the UC3637 is seen to contain the high-gain error amplifier and the main ingre-

dients of the PWM amplifier. Since we are looking for an output of 6A, an H-bridge power stage must be added. The motor current  $I_M$  is sensed by means of a low value resistor  $R_S$ , and the derived voltage  $V_C$  is used to complete the feedback loop. Not shown in the block diagram is the back-EMF voltage, the product of motor shaft speed and  $K_V$ , the motor speed constant. Since this term does not contribute to the dynamics of the current feedback loop, it has purposely been left out.

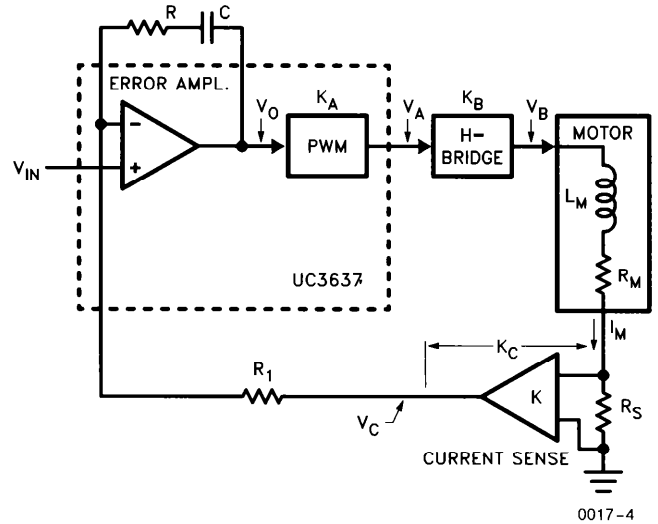


Figure 4. Block Diagram of the Complete Current-Control Loop

The transfer functions of the error amplifier and motor are as follows:

$$(3) \frac{V_O}{V_C} = - \frac{1 + sRC}{sR_1C}$$

$$(4) \frac{I_M}{V_B} = \frac{1}{R_M(1 + sT_M)}$$

where  $T_M = L_M / R_M$ , the motor's electronic time-constant ( $R_S$  is assumed to be low when compared with  $R_M$ ). The forward transfer function is, then:

$$(5) G(s) = \frac{-K_A K_B (1 + sRC)}{sR_1R_MC (1 + sT_M)}$$

For the feedback transfer functions, we have simply:

$$(6) H(s) = \frac{V_C}{I_M} = K_C$$

Thus, for the closed loop,

$$(7) \frac{I_M}{V_{IN}} = \frac{K_A K_B (1 + sRC)}{K_A K_B K_C (1 + sRC) + sR_1R_MC (1 + sT_M)}$$

If we make the time-constant RC equal to the motor's time-constant  $T_M$ , this becomes:

$$(8) \frac{I_M}{V_{IN}} = \frac{K_A K_B}{K_A K_B K_C + s R_1 R_M C}$$

$$(9) \frac{I_M}{V_{IN}} = \frac{1}{K_C (1 + s T_1)}$$

where,

$$(10) T_1 = \frac{R_1 R_M C}{K_A K_B K_C} = \frac{R_1 L_M}{K_A K_B K_C R}$$

By making  $RC = T_M$ , we have eliminated one of the transfer function poles. The resulting closed-loop response, described by (7) has a gain of  $1 / K_C$  from  $\omega = 0$  to  $\omega = 1 / T_1$ , and drops at  $-6$  db/octave thereafter.

**DESIGNING THE HARDWARE**

In designing circuits intended to handle power, it is customary to start with the output stage. This is surely due to the fact that the power stage is more demanding of the designer's attention and care, whereas the low level circuits are far more adaptable to the requirements of the chosen output configuration.

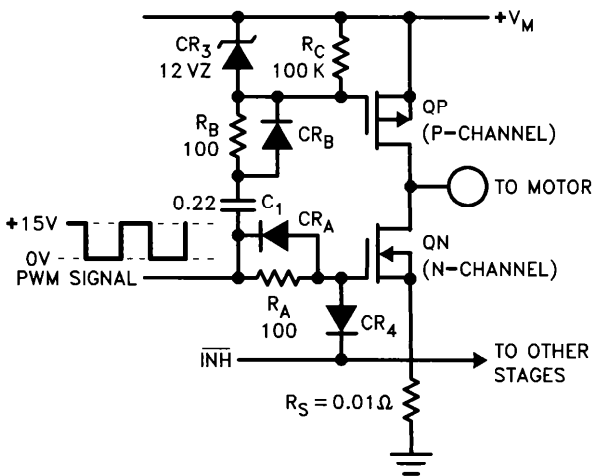
In the present case, power MOSFETs were chosen for the H-bridge because of their low losses, and because of their compatibility with the UC3637 outputs. Each totem-pole leg of the bridge is made up of one N-channel and one P-channel device. Such a pair can be driven in many different ways, of which several were considered for this particular design. The method that was finally chosen, shown in Figure 5, requires a few comments.

The first thing to notice is that the upper MOSFET, transistor QP, has its gate driven through a capacitor,  $C_1$ . This is not always practical of course, but in the case of a chopper drive combined with a stepping motor, it turns out that a driving signal is always present. At stand-still and at low speeds, it is the chopping rate that appears; at higher speeds, it is the stepping rate itself, or both. The driver is never required to deliver continuous DC (unchopped) to the motor winding, as it would to the armature of a brush-type DC motor at full speed. Consequently, QP never needs to be held in the ON state for more than a few microseconds, and for this the time constant of  $C_1 R_4$  is adequate. Also, resistor  $R_A$  in parallel with  $CR_1$ , together with the gate capacitance of QN, cause this transistor to turn off faster than it turns ON. Since the same thing is done for QP, the problem of cross-conduction is neatly taken care of. The Zener diode CR3 serves as a clamp for the QP gate voltage. Finally, an inhibiting line, INH, is provided as a protection for QP and QN during the power turn-on time, when the  $+V_M$  voltage is rising and  $C_1$  must be charged. An auxiliary circuit senses a positive  $dV_M/dt$  and holds the INH line low, thus keeping QN OFF during this time.

An important point in favor of this arrangement is that the gate-drive circuit losses are independent of  $V_M$  and so this voltage can be set anywhere within the  $V_{ds}$  rating of the power MOSFETs.

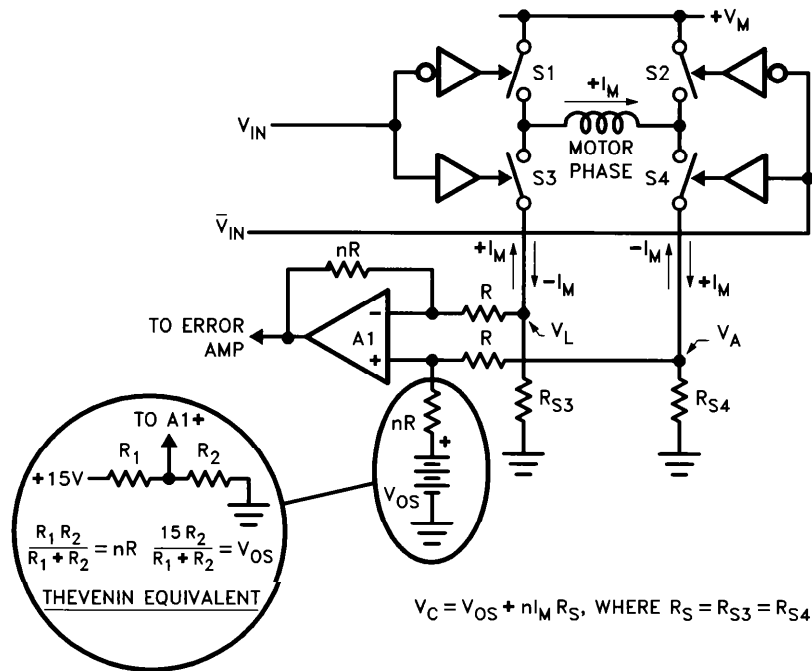
We can now consider the H-bridge with its motor winding load, as shown in Figure 6. The bridge is shown schematically with its driving circuits, but the action is still as shown in Figure 5. For example, when  $V_{IN}$  is high, switch S1 is OFF and S3 is ON, and so forth. Furthermore, the opposite side of the bridge is driven by the complementary signal  $V_{IN}$ . With  $V_{IN}$  low, S1 and S4 will be conducting, and the load current  $I_M$  will increase in the positive direction (indicated by the  $+I_M$  arrow). Similarly, when  $V_{IN}$  is high, both S2 and S3 conduct, causing  $I_M$  to increase in the negative direction. Remember that the load is inductive, and that inductance is an energy storing element. Therefore, if we have some positive  $I_M$ , due to S1 and S4 being closed, and we switch to S2 and S3 closed, the previous value of  $I_M$  will continue to flow "uphill," so to speak, while decreasing. At the time of switching, this current ceases to flow down through sense resistor  $R_{S4}$  to ground and starts flowing up through  $R_{S3}$  and back to the supply.

Switches S1 through S4 are able to conduct in either direction when in the ON state—a very neat feature of power MOSFETs. Furthermore, their intrinsic diode protects the devices from reverse voltage pulses during the switching no-overlap transition. Since we wish to control this current very closely in both magnitude and direction, it is



0017-5

Figure 5. Totem-Pole Leg of Output H-Bridge



0017-6

Figure 6. H-Bridge Configuration with Bidirectional Current Sensing

now necessary to generate a voltage  $V_C$  that gives an accurate indication of the current  $I_M$  over the full range from maximum positive to maximum negative. This is done by the circuit section of Figure 6 which includes the op-amp A1.

In that circuit, the voltage  $V_{OS}$  is meant to offset the output  $V_C$  of A1 to some chosen value that will correspond to  $I_M = 0$ . The value of  $V_C$  can be written as:

$$(11) V_C = V_{CS} + nI_M R_S$$

This offset is necessary when the design requires a single polarity supply, as in our case. When two supply polarities are available for the control circuit, one can simply make  $V_{OS} = 0$ . For the single supply case, the  $nR$  and  $V_{OS}$  combination is implemented by a simple resistor divider from  $\pm V_{CC}$  to ground (a Thevenin equivalent) of the required impedance and open voltage.

To keep the circuit losses to a minimum, we should use low values for the sense resistors  $R_{S3}$  and  $R_{S4}$ . Yet, they need to be accurate and temperature-stable. In our case, having decided on a  $V_C$  scale of 0.5V per motor ampere, we have selected  $R_S = 0.1 \Omega$  and a current sense amplifier gain  $n = 5$ . We have also set  $V_{OS} = V_{CC}/2 = 7.5V$ , so that we will have  $V_C = 7.5 + 0.5 I_M$ . This means that as the current  $I_M$  varies from + 6A to -6A, the analog voltage  $V_C$  will vary from + 10.5V to + 4.5V. At  $I_M = 0$ ,  $V_C$  will be equal to 7.5V.

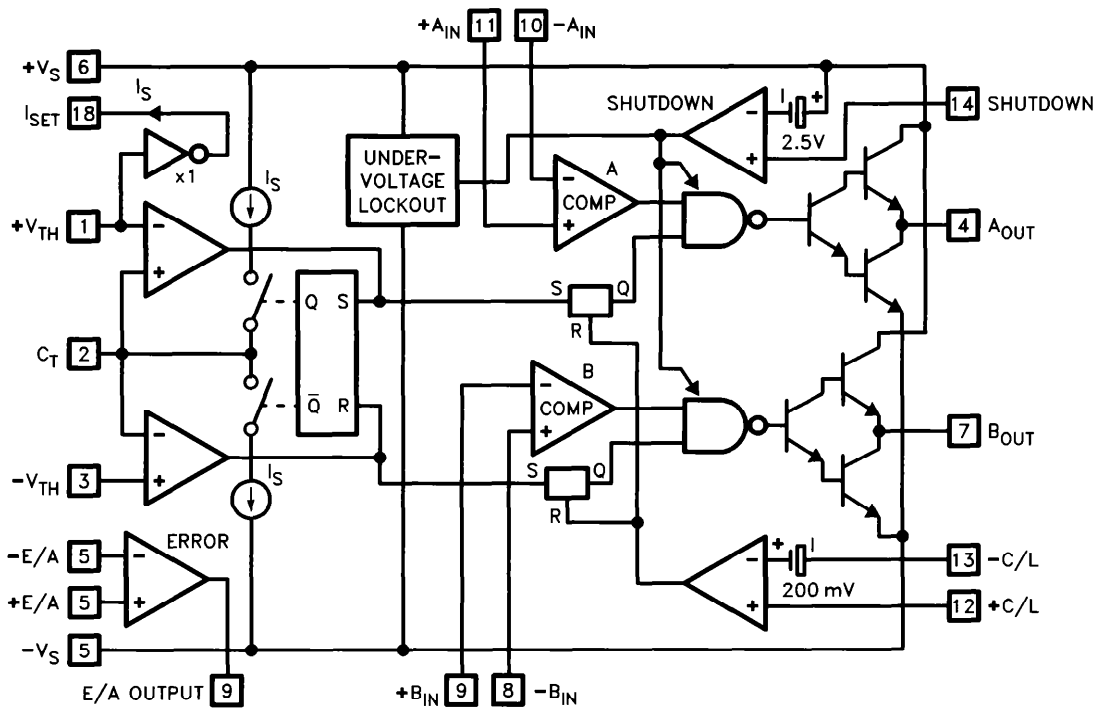
### SETTING UP THE PWM CONTROLLER

Having designed the power output stage (H-bridge) and the current-sense circuit, we can proceed to the PWM controller (UC3637) and its external components. The device itself has been described in great detail in its data sheet and in an application note (Publication U-102, available from Unitorde Integrated Circuits Corporation).

In the present design, we use the UC3637 to generate the two H-bridge driving signals  $V_{IN}$  and  $\bar{V}_{IN}$ , at the device's output pins 7 and 4, respectively.

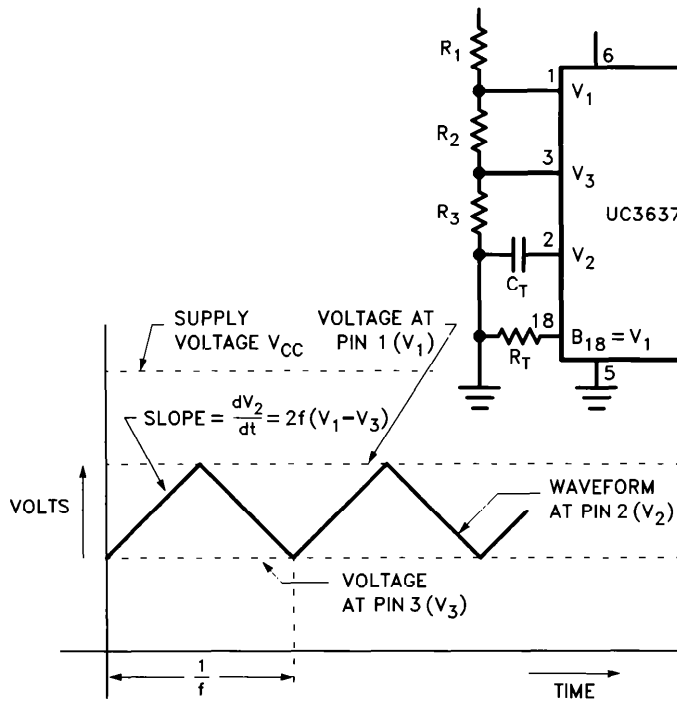
Figure 7 shows in block form the internal workings of the device. Since operation from a single + 15V supply is desired, pin 5 will be GROUND and pin 6 will be + 15V. We selected, for the ramp oscillator, a waveform as shown in Figure 8, which fits well in the + 15V headroom given by our  $V_{CC}$  supply. The formulas given in Figure 8 show how the various components are calculated.

Next, we set up the two PWM comparators by tying the inverting inputs (pin 10) of the A comparator, and the non-inverting input (pin 8) of the B comparator together and apply the ramp (pin 2) to this line. The remaining comparator inputs (pins 9 and 11) are next connected together to become the PWM input point. It can be seen from the block diagram of Figure 7 that as the control voltage applied to this point varies from + 5V to + 10V, the duty cycle of the output at pins 4 and 7 also varies.  $V_4$  and  $V_7$  are complementary signals; and the voltage swing of each of these signals is from a low value between 0V and + 2V, and a high value between  $(V_{CC} - 2V)$  and  $V_{CC}$ .



0017-7

Figure 7. Block Diagram of the UC3637. The two outputs can drive power MOSFETs directly.



0017-8

$$f = \text{ramp frequency}$$

$$I_T = \frac{V_{18}}{R_T} = \frac{V_1}{R_T} \text{ (should be about 0.5 mA)}$$

$$\text{then, } R_T = 2000 V_1 (\Omega)$$

$$C_T = \frac{250 \times 10^{-6}}{f(V_1 - V_3)} (\text{fd})$$

Figure 8. Setting up the ramp oscillator requires only five external components.

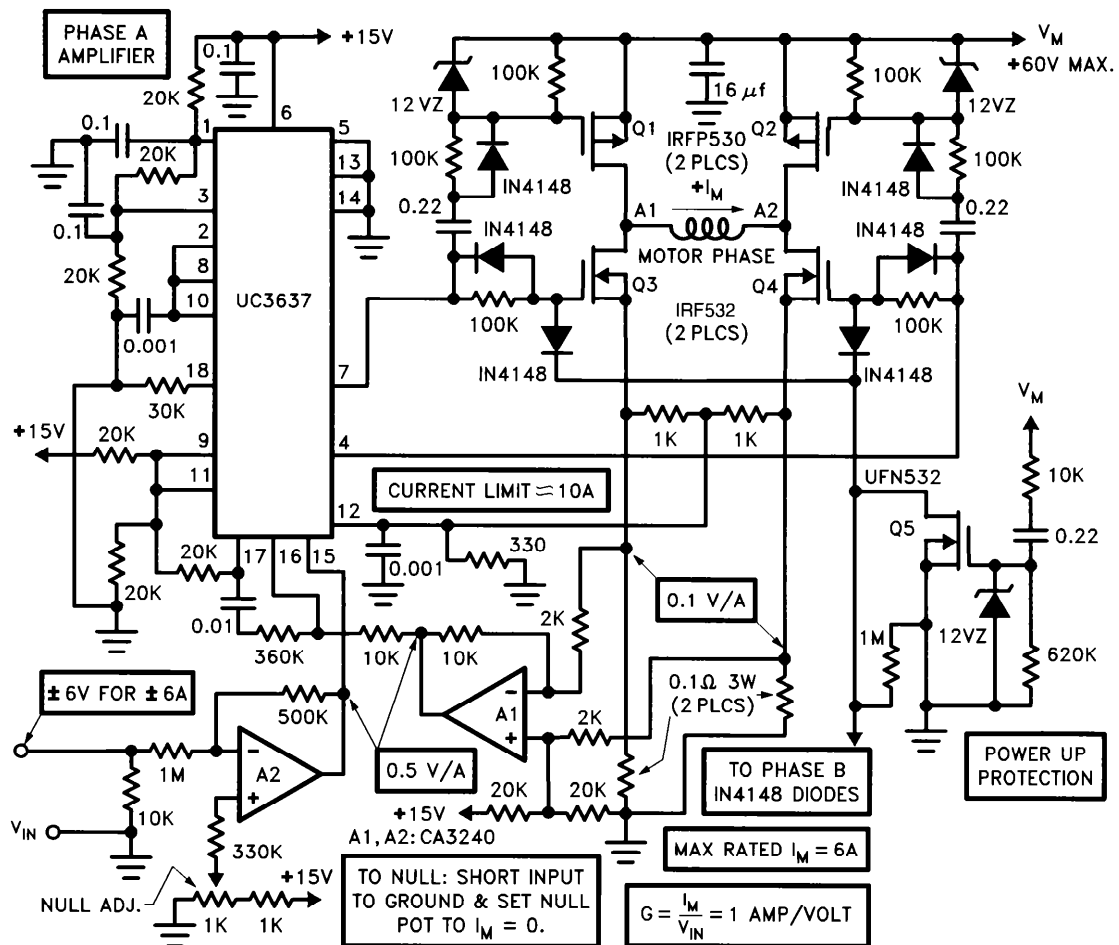


Figure 9. PWM Transconductance Amplifier UC3637

0017-9

The error amplifier is used as a source for the control signal. But because its output (pin 17) has a voltage range greater than the +5V to +10V range of the  $V_C$  ramp signal, and we want to prevent the modulation range from ever reaching 0% or 100% (because of the capacitively coupled P-channel MOSFET devices) we add a simple resistive network consisting of three equal resistors to serve as an attenuator. The final result can be seen in the complete schematic of Figure 9.

### CURRENT LIMIT AND CONTROL

The current limit feature of the UC3637 is used to protect the output transistors and motor from excessive current (6A in this case). As the block diagram of Figure 7 shows, the current limit comparator (pins 12 and 13) of the UC3637 is internally biased to a threshold of 200 mV. The network that connects the two sense resistors to pin 12, consisting of two 1K and one 330 $\Omega$  resistors, causes a voltage of 200 mV to appear at pin 12 when the voltage at either sense resistor is about 1V, corresponding to a

current of 10A. Consequently, the maximum output current will be limited to 10A. The current feedback loop is closed by feeding the output of the current sense amplifier to pin 16, the inverting input of the error amplifier of the UC3637. An RC time constant of 3.6 msec is used for the zero in this amplifier's transfer function (equations 8, 9, and 10) which is close to the effective electrical time constant of the motor. Also, a level-shift circuit is provided by means of op amp A2 to permit the use of a control input centered at zero volts, and a control range from -6A to +6A. The circuit allows this even though the op amp is powered by a single positive supply.

### TEST RESULTS

The design circuit, shown in Figure 9, was breadboarded for testing at Unirode and also at Portescap. The assembly includes two amplifiers, one for each motor phase and a "power on" auxiliary circuit for protection of the power MOSFETs. The output devices are equipped with small sheet metal heat sinks.

The circuit draws about 65 mA from the + 15V supply. The power output section operates with a supply ranging from +20V to + 60V, with no damage occurring if this voltage is lower than + 20V.

The circuit performed very well, with excellent linearity and phase matching. The various plots taken, showing output current versus input voltage, are quite straight, and the transconductance is accurate to within 1%. Furthermore, the PWM frequency was subsequently increased to slightly above 100 KHz (by reducing  $C_T$ ) and the performance re-checked. The result was a marked increase in motor efficiency, due to reduced current ripple, with all other results remaining excellent.

## CONCLUSION

Microstepping is a technique of considerable interest in the design of many products, particularly those in which the lower cost of open-loop positioning is an essential parameter. A motor such as Portescap's Model P-750, with its accurately sinusoidal torque curve, becomes even more attractive once its microstepping driver is shown to be fairly simple and inexpensive. The end result is not only precise open loop positioning, but quiet operation, freedom from resonance problems, and excellent electrical efficiency. Incidentally, the motor is available with two quadrature speed sensing coils that can be used for speed and position control, if desired.